Journal of Environmental Chemical Engineering 9 (2021) 106845

Contents lists available at ScienceDirect

Journal of Environmental Chemical Engineering

journal homepage: www.elsevier.com/locate/jece

Synthesis of Ag nanoparticles from waste printed circuit board

Marcos Paulo Kohler Caldas [a], Thamiris Auxiliadora Gonçalves Martins [b,*], Viviane Tavares de Moraes [c], Jorge Alberto Soares Tenório [b], Denise Crocce Romano Espinosa [b]

[a] Federal Institute of Education, Science and Technology of Espirito Santo (IFES), Rodovia ES-010, Km 6.5, Manguinhos, CEP 29173-087 Serra, ES, Brazil
[b] Department of Chemical Engineering, Polytechnic School of the University of Sao Paulo (USP), Lago St., N° 250, CEP 05508-080 Sao Paulo, SP, Brazil
[c] Maua Institute of Technology, Praça Maua, 1 - Maua, Sao Caetano do Sul CEP 09580-900, SP, Brazil

ARTICLE INFO

Editor: Teik Thye Lim

Keywords:
Recycling WPCBs
Memory boards
Silver precipitation
Silver nanoparticles

ABSTRACT

The amount of waste from electrical and electronic equipment has been growing every year. The printed circuit boards contained in this waste include metals that can be recovered through urban mining, adding value to this waste and minimizing environmental impacts with its incorrect disposal or treatment. In this work, memory boards obsolete with 0.053 wt% Ag were used. The extraction of all metals studied (Ag, Al, Cu, Fe, Ni, Sn, and Zn) involved the evaluation of the Pourbaix and speciation diagrams to identify the pH and redox potential conditions, considering the possible species formed with leaching agents: sulfuric, nitric, and hydrochloric medium. After the definition of the leaching agent, the extraction routes by hydrometallurgical processing were proposed from the parameters of temperature, s/l ratio, and reaction time previously studied. Route A was composed of sequential stages (the first leaching in a sulfuric medium and the second in an oxidizing sulfuric medium) and obtained 100% of Ag recovery. Route B consisted only of leaching in an oxidizing sulfuric medium, obtained about 94% of the Ag recovery, and could not contribute to the subsequent purification steps (if necessary) of this solution, as all metals would also be in the solution. These two routes showed that Ag can only be recovered in an oxidizing sulfuric acid medium, according to the conditions studied. Ag recovered in the leach liquor of the second stage of Route A was purified by chemical precipitation with NaCl, and the AgCl was solubilized in an NH_4OH solution. This solution was used to synthesize silver nanoparticles by the Turkevich method in 25 min. The spherical nanoparticles synthesized an average size distribution of 67 nm.

1. Introduction

The Circular Economy (CE) concept is based on continuous growth and increased resource production, with the objective of making systems sustainable through long-term design, maintenance, repair, reuse, remanufacturing, reconditioning, and recycling. Waste electrical and electronic equipment (WEEE) is considered one of the challenges and opportunities of mining municipal waste within this context of CE [1,2]. Estimates state a total generation of these wastes will be 52.20 million tons (6.8 kg. inhabitant^{-1}) in 2021 and 74.7 million tons in 2030 [2–4]. Waste Printed Circuit Boards (WPCBs) represent about 10% of that amount produced [2]. The PCBs have about 30% of your total weight metals, such as copper, iron, tin, nickel, lead, zinc, silver, gold, palladium, and for this reason its waste is considered a source of funds for urban metal mining [2,5–8].

In this context about the amount of metals that are present in these WEEE, Havlik et al. cite that they can contain 115–280 ppm of Ag while the ore has from 5 to 7 ppm [9]. One ton of WPCBs can contain up to 1500 g of Au (800 times the amount of Au in Fe ore - USA) and 210 kg of Cu (40 times the concentration of Cu in Cu ore - USA) [10]. Therefore, the recycling of these residues becomes important both for the preservation of the environment and for the recovery of secondary materials [11–13].

There are several techniques and technologies for the recovery of these metals from WPCBs, such as mechanical processing, pyrometallurgy, hydrometallurgy, and biotechnology. Hydrometallurgical routes can be selective for metals in low concentrations, and they have lower energy consumption and gas emissions when compared to pyrometallurgy. The liquor resulting from the hydrometallurgical process of the WPCBs needs subsequent purification steps as it has several metals in solution due to the complexity and heterogeneity of these wastes [14–17]. Several reagents can be used to leach and recover the precious

* Corresponding author.
E-mail address: thamirisagm@usp.br (T.A.G. Martins).

https://doi.org/10.1016/j.jece.2021.106845
Received 18 June 2021; Received in revised form 16 November 2021; Accepted 17 November 2021
Available online 24 November 2021

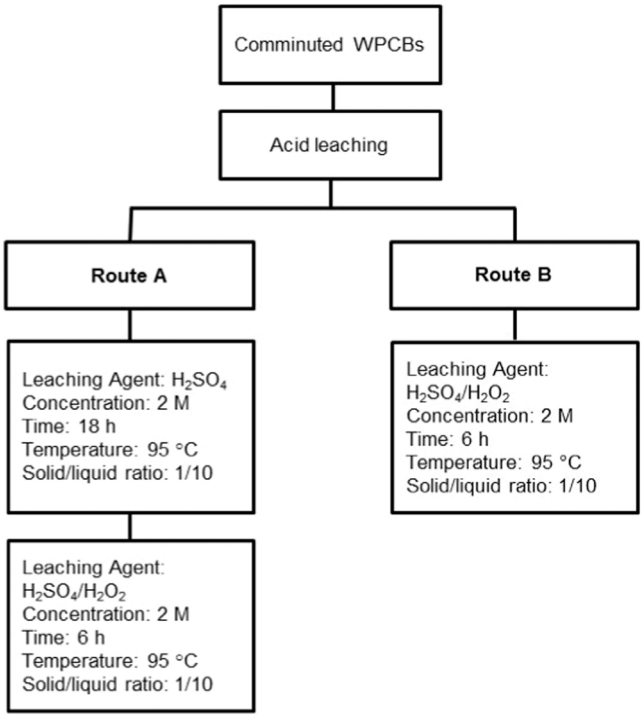

Fig. 1. Flowchart of the PCB hydrometallurgical process for routes A (with 1st step in H_2SO_4, 2 M, 18 h, 95 °C, s/l ratio 1/10 and the 2nd in H_2SO_4 2 M + H_2O_2, 6 h, 95 °C, s/l ratio 1/10) and B (H_2SO_4 2 M + H_2O_2, 6 h, 95 °C, s/l ratio 1/10).

Table 1
Leaching conditions observed in the individual Pourbaix diagrams of each metal can favor their obtaining in the ionic phase (at 95 °C).

Leaching conditions - obtaining the metal in the ionic phase at 95 °C		
Element	pH range	Eh (mV) range
Cu^{2+}	0–2.3	350–2000
Fe^{2+}	0–5.0	- 500–700
Ag^{1+}	0–5.5	750–1250
Al^{3+}	0–6.0	-100–2000
Sn^{2+}	0–0.5	-100–0
Zn^{2+}	0–4.3	-750–2000
Ni^{2+}	0–8.3	-200–2000

metals (such as Au and Ag) from these wastes, such as aqua regia, cyanide, thiourea, halogens, and thiosulfate [18–20].

Aqua regia offers difficulties to be used on an industrial scale due to its oxidation properties and high corrosion of metal piping and equipment. The use of cyanide can lead to damage to health and the environment, due to its toxicity [21–24]. Thiosulfate is a reagent with less environmental impact and low value when it is compared to cyanide [18,24,25], but its leaching efficiency is lower than cyanide, and a greater amount of reagent is used to obtain the same rate of extraction efficiency [23,26]. In addition, another disadvantage is that the thiosulfate stability decreases with increasing temperature and at acid pH values [19,23]. The thiourea used as a leaching agent, on the other hand, presents as its main disadvantages its high cost and easy oxidation (at alkaline pH) when compared to cyanide [23,26]. Studies also report that thiourea may be a carcinogenic compound [24,27].

The application of inorganic acids (such as H_2SO_4, HNO_3, and HCl) has also been an option for replacing these reagents for metal recovery [28–30]. Petter et al. [18] used HNO_3 in a proportion of 1/3 in relation to deionized water, at 60 °C, for 2 h, with a solid/liquid ratio of 1/20, and they obtained about 3.5 g of Ag/ton from mobile phones WPCBs [31]. Khaleghi et al. performed Ag recovery from copper anode slime,

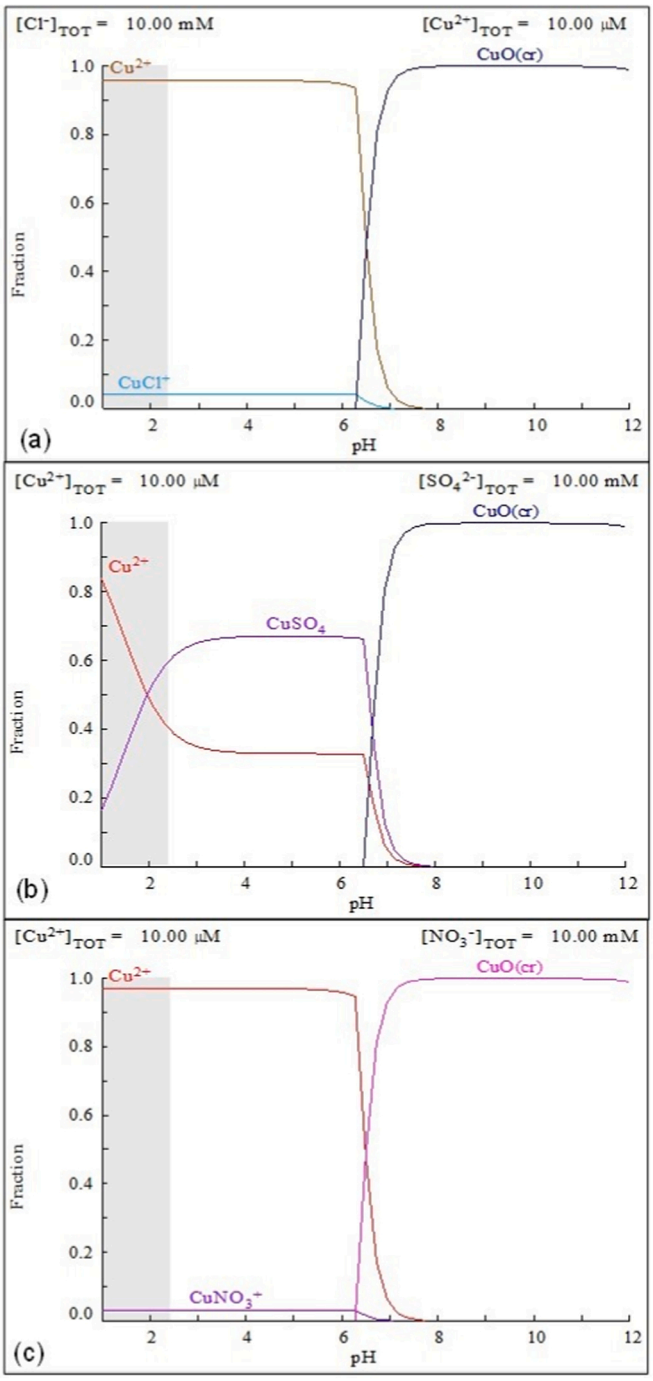

Fig. 2. Cu (10 µM) speciation in medium (10 mM) a) hydrochloric, b) sulfuric, and c) nitric, adapted from Software Hydromedusa.

with different concentrations of H_2SO_4 and HNO_3, temperatures (25, 40, 60, and 90 °C) and with agitation of 1000 r/min. Almost 96% of the Ag can be extracted with nitric acid (4 M) at atmospheric pressure, 90 °C, for 3 h while sulfuric acid (16 M), 90 °C, for 3 h, leached 26% of Ag [32]. Yi et al. studied the recovery of Ag from photovoltaic modules, with 1, 2, and 3 M of the leaching agents: HCl, H_2SO_4, and HNO_3, 1/5 by weight to solid/leachate ratio, for 2 h, at 20–40 °C. Nitric acid (3 M) was able to remove more than 80% of Ag from the studied wastes [33]. In tests for Ag recovery from dental amalgam wastes, Yilmaz et al. leached 50% HNO_3 in a solid/liquid ratio of 1/5, for 4 h and room temperature, and their results showed that silver leaching efficiency was above 99.8% and leach solution contained 16 g/L Ag^+ [34]. Xing and Lee (2017)

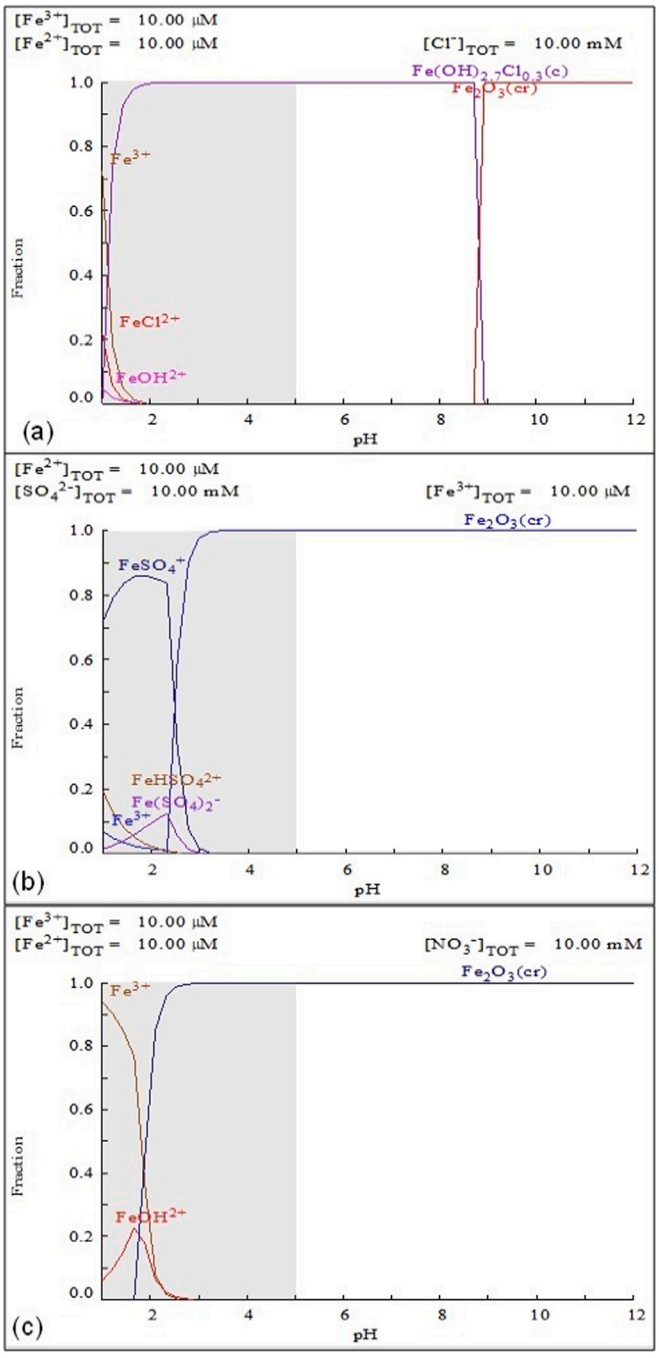

Fig. 3. Fe (10 µM) speciation in medium (10 mM) a) hydrochloric, b) sulfuric, and c) nitric, adapted from Software Hydromedusa.

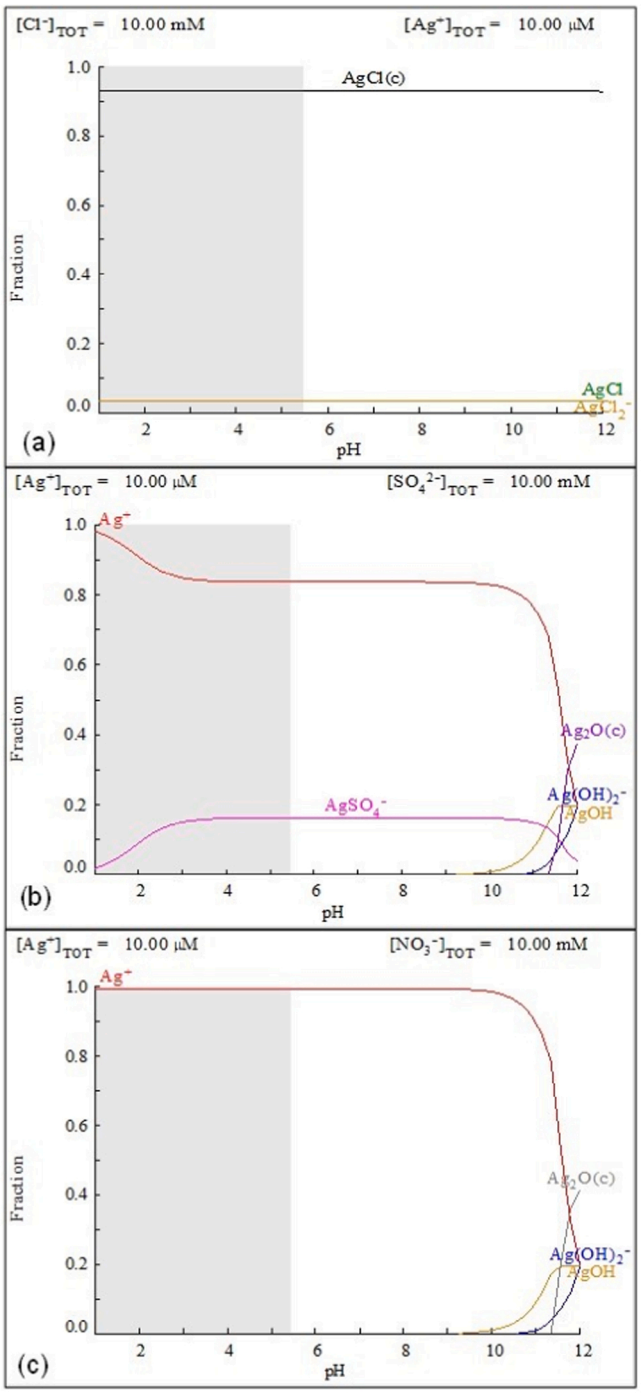

Fig. 4. Ag (10 µM) speciation in medium (10 mM) a) hydrochloric, b) sulfuric, and c) nitric, adapted from Software Hydromedusa.

performed tests for the recovery of gold and silver from anode slime resulting from the treatment of copper sludge, by leaching the slime with a mixture of HCl and oxidizing agents (H_2O_2, NaClO and HNO_3). According to the results obtained, the percentage of Ag leaching was only 10% with the mixture of HCl and H_2O_2 or NaClO, while 28% from Ag were dissolved in the mixture of HCl and HNO_3 [35]. Behnamfard et al. performed the selective recovery of Cu, Ag and Au from WPCBs, from consecutive leaching stages: in sulfuric acid in the presence of H_2O_2, in which 99% of the copper content was solubilized, and the dissolution of about 86% Au and 71% Ag was obtained in another stage with acid thiourea in the presence of ferric iron as an oxidizing agent [36]. Andrade et al. used two different types of WPCBs (memory board and motherboard) to extract Ag through a hydrometallurgical route based on only one stage of leaching in an oxidizing medium. They used H_2SO_4 (2 M, s/l ratio 1/20, 95 °C, for 12 h) with the addition of H_2O_2 (35%) every 15 min. Thus, an 83% Ag recovery was obtained on the motherboards and 33% on the memory boards [37]. Martins et al. were able to extract more than 84% of Ag (out of a total of 0.052 wt%) from motherboards in 3 h of oxidizing sulfuric acid leaching that occurred after a first one in the sulfuric acid medium [38].

The recovered metal can be reused as a material resource and reinserted in the production of new products/materials such as metallic nanoparticles [39–41]. Nanotechnology is a new field in science, and it is seen as the future in the development of new materials for the most diverse applications. Metallic nanoparticles may have antimicrobial,

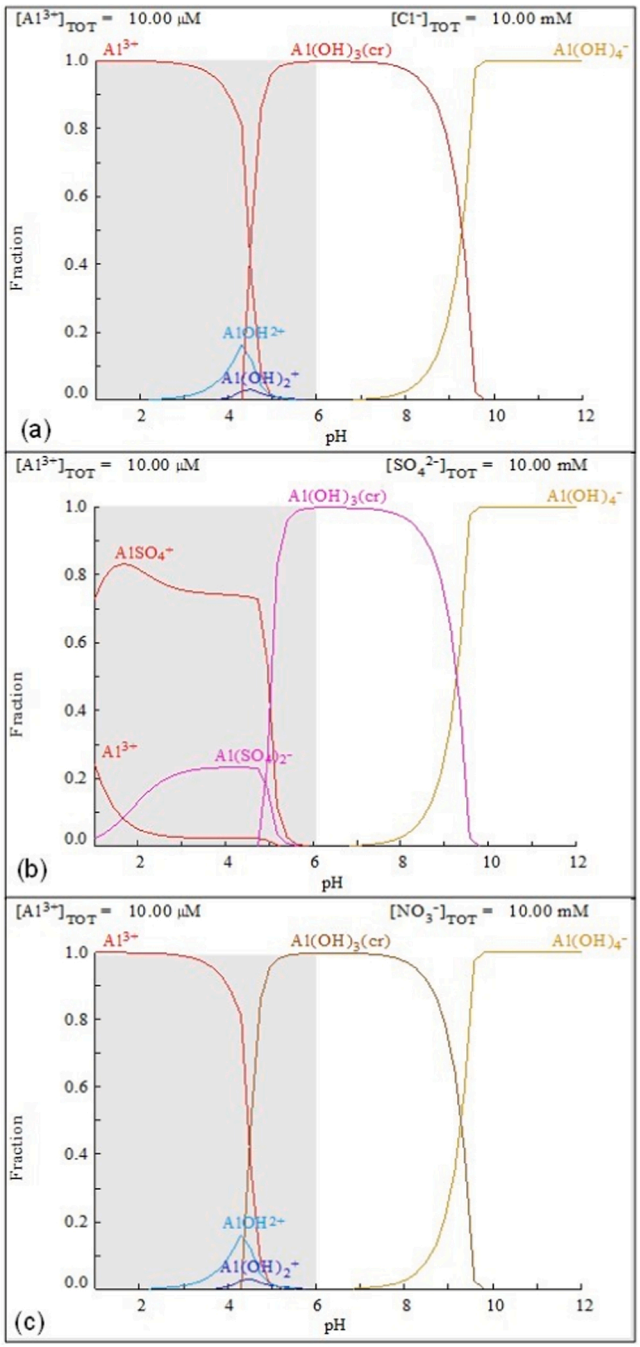

Fig. 5. Al (10 µM) speciation in medium (10 mM) a) hydrochloric, b) sulfuric, and c) nitric, adapted from Software Hydromedusa.

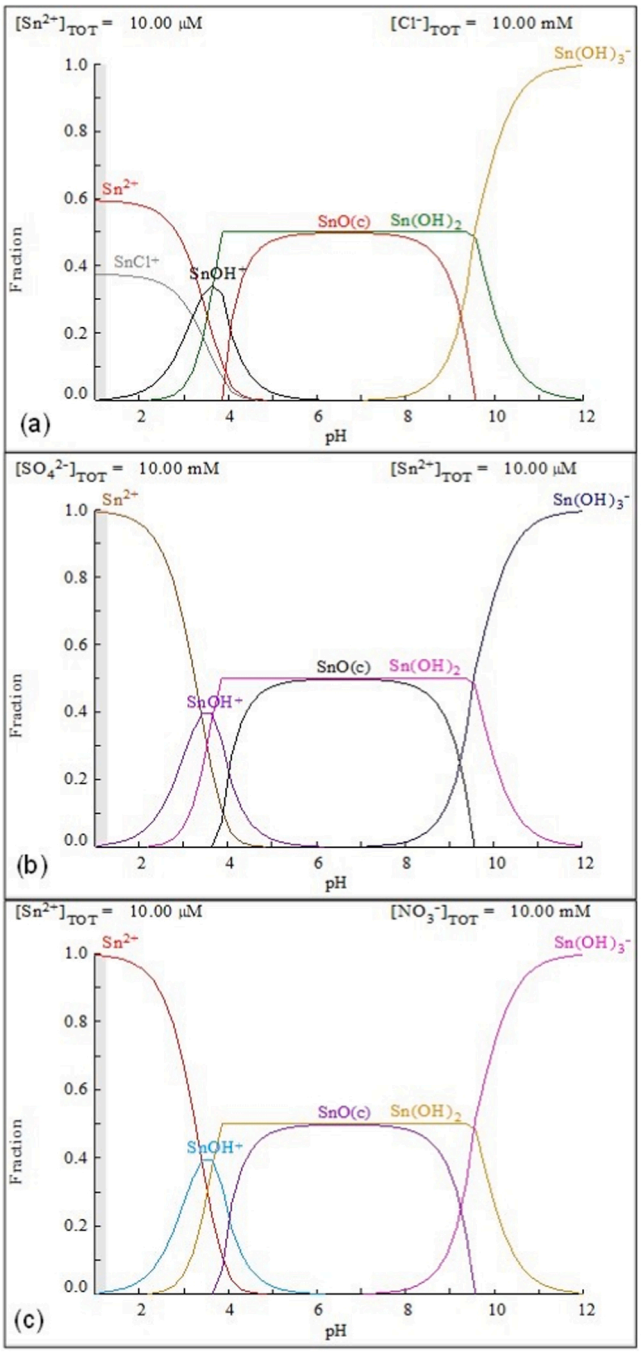

Fig. 6. Sn (10 µM) speciation in medium (10 mM) a) hydrochloric, b) sulfuric, and c) nitric, adapted from Software Hydromedusa.

dental treatment, wound healing, surgery work, catalyst, and biomedical applications [42]. The bactericidal and fungicidal properties of silver nanoparticles (AgNPs) are its most industrially exploited characteristics, being a product relatively widespread in the market [43–46]. The application of AgNPs synthesized from the recovery of Ag from wastes can be restricted concerning items such as food products and medicines, so studies such as toxicity must be carried out before their use.

Swain et al. recovered Ag from waste generated during manufacturing of low temperature co-fired ceramic for synthesis of nanoparticles with about 100 nm size using $NaBH_4$, Polyvinylpyrrolidone (PVP), and Polyethylene glycol (PEG). The extraction was also carried out with HNO_3 and precipitation through the use of HCl (Ag was precipitated as 83.45%) [20]. Khaleghi et al. performed the recovery of Ag from anode slime by leaching in HNO_3, and they realized the purification of the Ag from the leach solution with addition of HCl. Thus, the Ag was precipitated as AgCl, and, subsequently, the compound was dissolved using an ammonia solution. After the recovery and dissolution of Ag, they synthesized uniform 12 nm Ag nanoparticles by the chemical reduction method also with the use of $NaBH_4$ and N_2H_4 as a reducing agent [32].

The present paper shows a route for the recovery of metals (with a focus on Ag) from obsolete printed circuit boards of the memory board type. From the individual study of speciation and Pourbaix diagrams of each metal in three acids commonly used for hydrometallurgical leaching processes: hydrochloric, sulfuric, and nitric. The results presented show several possibilities for the selective leaching of metals

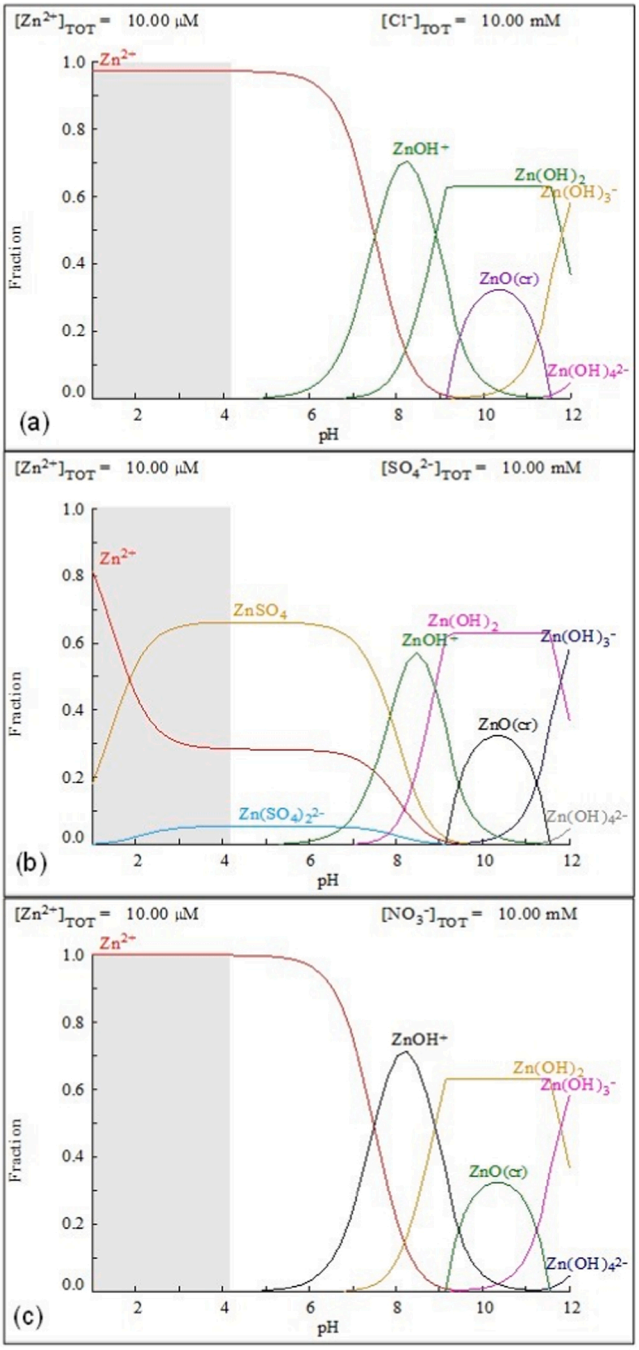

Fig. 7. Zn (10 µM) speciation in medium (10 mM) a) hydrochloric, b) sulfuric, and c) nitric, adapted from Software Hydromedusa.

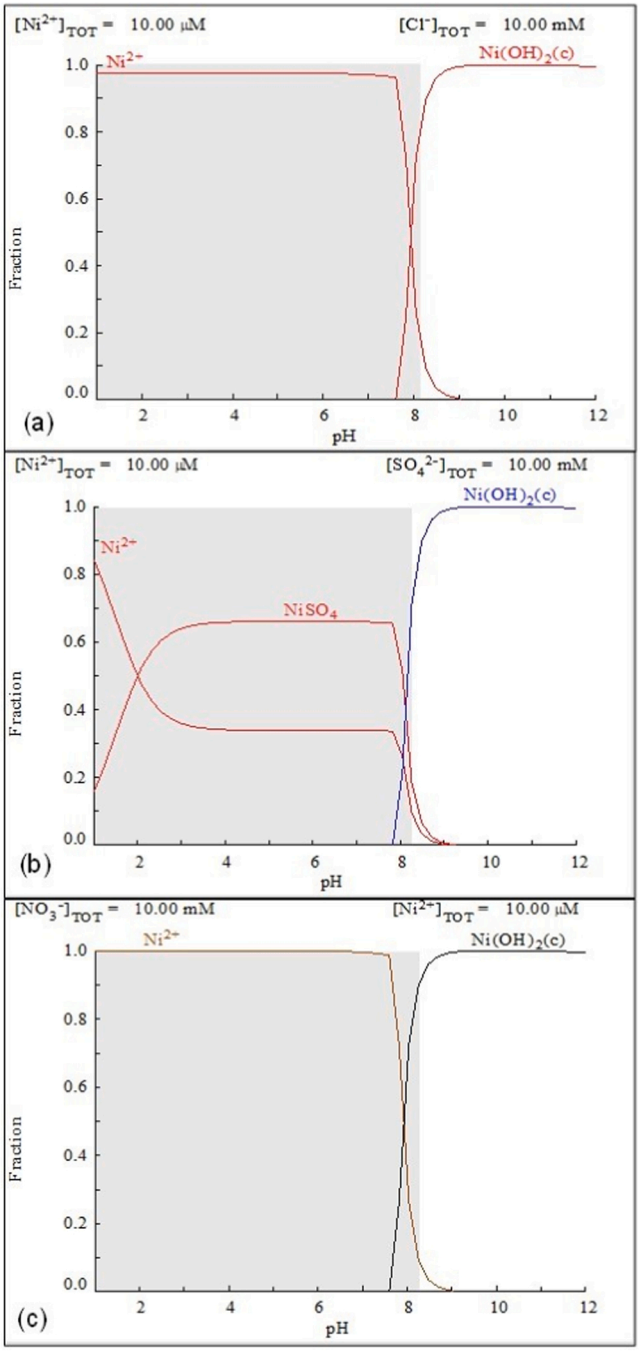

Fig. 8. Ni (10 µM) speciation in medium (10 mM) a) hydrochloric, b) sulfuric, and c) nitric, adapted from Software Hydromedusa.

present in these residues according to the values of pH and potential redox (ORP). From this study, the leaching agent was defined, and two hydrometallurgical routes were tested where all the Ag was extracted. The purification of this solution extraction was realized by the chemical precipitation method, and Ag nanoparticles (AgNPs) were synthesized although a traditional method of preparation using sodium citrate (Turkevich method). Thus, the focus of the present work was not to carry out the study of parameters (temperature, time, concentration, solid and liquid relationship, and kinetics) of the routes studied for the recovery of metals from WPCBs and parameters of the synthesis of nanoparticles, but to present a complete route of the recovery, purification, and synthesis of nanoparticles, to add value to the recycling of these residues and show the potential of urban mining.

2. Experimental procedure

2.1. Reagents and solutions

All reagents were used of analytical grade, without further purification. Ultrapure water was used to prepare solutions, and the synthesis was not carried out in an inert atmosphere.

2.1.1. Metals characterization from WPCBs

The metals of the WPCBs (memory boards) were characterized according to Yamane et al. [47], and this study was carried out in the previous work presented by Andrade et al. [37]. According to Andrade et al., the scraps were disassembled, crushed, using a knife and hammer

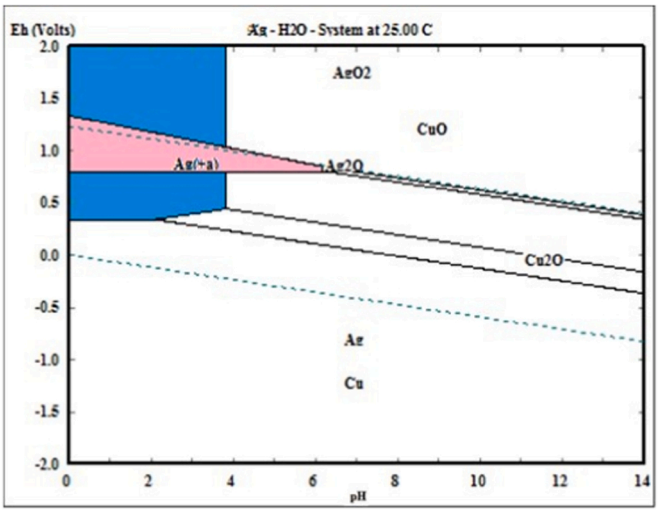

Fig. 9. Pourbaix Diagram: system Ag–H_2O and system Cu–H_2O, 25 °C, adapted from Software HSC Chemistry 7.1.

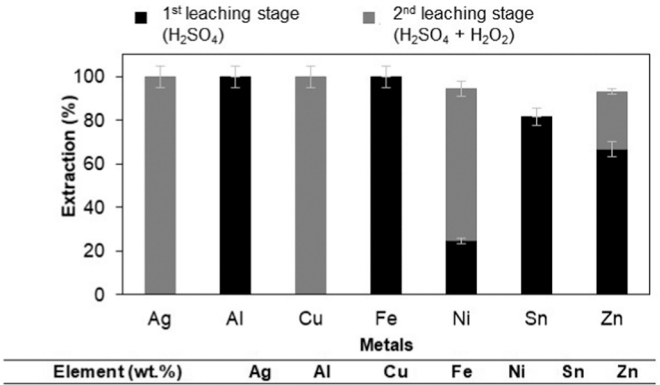

Element (wt.%)	Ag	Al	Cu	Fe	Ni	Sn	Zn
1st leaching stage	0.0	0.0	0.0	100.0	24.6	81.6	66.8
2nd leaching stage	100.0	0.0	100.0	0.0	69.7	0.0	26.3
Total extraction Route A	100.0	100.0	100.0	100.0	94.3	81.6	93.1
Total extraction Route A (g metals/100 g WPCBs)	0.053	1.430	13.83	1.47	0.302	1.387	0.040

Fig. 10. Mass percentage of leached metal from the WPCBs for each leach stage determined by ICP-OES, Route A (1st step in H_2SO_4, 2 M, 18 h, 95 °C, s/l ratio 1/10 and the 2nd in H_2SO_4 2 M + H_2O_2, 6 h, 95 °C, s/l ratio 1/10).

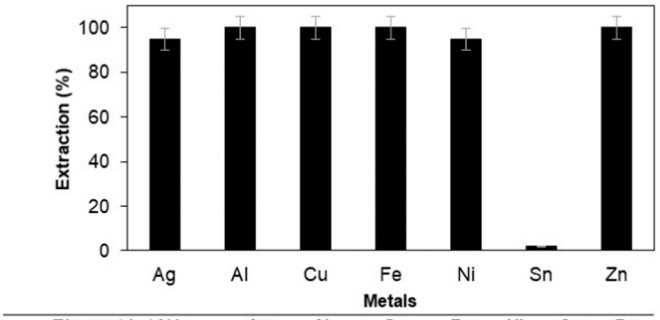

Element (wt.%)	Ag	Al	Cu	Fe	Ni	Sn	Zn
Total extraction Route B	94.8	100.0	100.0	100.0	95.0	2.1	100.0
Total extraction Route B (g metals/100 g WPCBs)	0.050	1.430	13.830	1.47	0.304	0.036	0.043

Fig. 11. Mass percentage of leached metal from the WPCBs by ICP-OES, Route B (H_2SO_4 2 M + H_2O_2, 6 h, 95 °C, s/l ratio 1/10).

Table 2
The ORP and pH were measured at the end of each stage of Route A (1st step in H_2SO_4, 2 M, 18 h, 95 °C, s/l ratio 1/10 and the 2nd in H_2SO_4 2 M + H_2O_2, 6 h, 95 °C, s/l ratio 1/10).

Leaching stage	ORP (V)	pH
1st (H_2SO_4)	0.465	-0.5
2nd (H_2SO_4 +H_2O_2)	0.717	0.1

mill, and chemical digestion was performed: crushed scrap was added in aqua regia (solid/liquid ratio 1/20), for 24 h. This solution was filtered and the digestion liquor with the solubilized metals was obtained. The quantification of the main metals of the digestion liquor (Ag, Au, Al, Cu, Fe, Ni, Sn, and Zn) was performed by inductively coupled plasma-optical emission spectrometry (ICP-OES) [37].

2.2. Metals extraction

The extraction of the metals was carried out through hydrometallurgical processing. The speciation and Pourbaix diagrams (Fig. 1S –7S in Supplementary Material) of the metals quantified were individually evaluated to verify the type of acid, pH, and potential for the extraction of the metals of interest, with a focus on the recovery of the Ag. Just to evaluate the behavior of metals in solution, the concentration considered for each acid was 10 mM, and metals were 10 μM. Thus, after analyzing the diagrams, two routes (A and B) were studied under constant mechanical agitation in a closed system. Fig. 1.

The flowchart of Fig. 1 details the leaching steps in which the concentration and leaching agent, the time, the temperature used, and the solid/liquid ratio are presented. Route A consists of two stages in which the first was the selective leaching of Fe and the second for recovery of Ag. Route B was composed of a single leaching step.

After each leaching step of each route, a 50 mL aliquot of the liquor was removed for chemical analysis (in triplicate) at ICP-OES. The leached liquor corresponding to each of these steps was filtered, and the material retained was washed with high purity water and dried in an oven for 24 h at 60 °C. Finally, the weighing of the non-leached material was carried out. After this weighing, this dry waste obtained was subjected to the next leaching.

The parameters for metal leaching of WPCBs used were defined from the studies by Silvas et al. who investigated the metallic recovery of printer WPCBs also using two leaching steps, the first only in sulfuric acid (s/l ratio 1/10, at 75 °C, 4 h) and the second with sulfuric acid and addition of hydrogen peroxide. However, at the end of the two steps, not all the Ag present in the studied WPCBs was extracted in the proposed process [48]. Thus, in the current study, the temperature and time were modified to ensure maximum extraction of the metals present in the study scrap.

2.3. Routes of the hydrometallurgical process

Hydrometallurgical processing was divided into two sequential stages of leaching in Route A: acid leaching in sulfuric medium and acid leaching in sulfuric and oxidizing medium. In acid leaching in sulfuric medium, the waste was leached for 18 h, sulfuric acid 2 M, solid/liquid ratio 1/10 (100 g WPCB/1000 mL acid), at 95 °C. After filtration and drying, the dry waste from this step was subjected to the second leaching. During leaching in sulfuric medium (2 M), 15 mL of hydrogen peroxide (130 volumes) were added every 15 min for 6 h of leaching.

Route B was composed of the second stage of leaching of Route A (acid leaching in a sulfuric and oxidizing medium), with the same concentration of acid, peroxide quantity, temperature, solid/liquid ratio, and ration time.

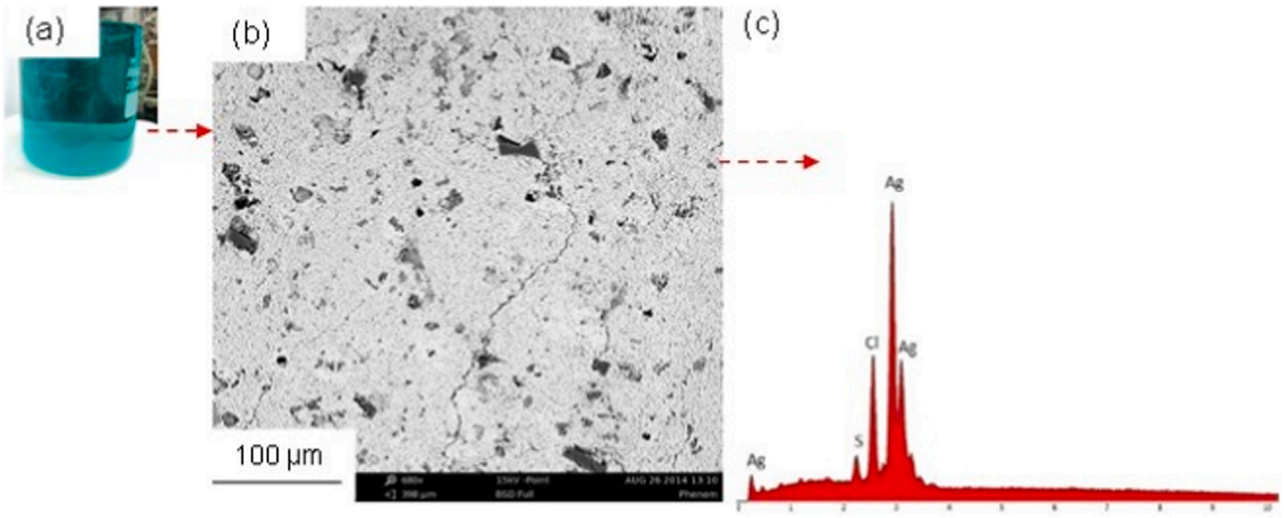

Fig. 12. a) Precipitate formed in the metal extraction solution of the WPCB sample, Route A (1st step in H_2SO_4, 2 M, 18 h, 95 °C, s/l ratio 1/10 and the 2nd in H_2SO_4 2 M + H_2O_2, 6 h, 95 °C, s/l ratio 1/10), b) Image obtained by backscattered electrons (SEM) of the AgCl precipitate present in the membrane on the filtration, c) EDS spectrum obtained from the area analyzed in the SEM of the precipitate formed on the filtration membrane.

Table 3
Parameters and appearance of the solution in AgNP synthesis tests.

Volume in added sodium citrate (mL)	Hot shake time (min)	Aspect of the solution
5	15	Translucent
	25	Translucent
10	15	Translucent
	25	Yellow
15	15	Turbid
	25	Precipitate formation

2.4. Purification of silver

The purification of the Ag recovery solution from the second stage of Route A was carried out utilizing chemical precipitation for subsequent synthesis of silver nanoparticles (AgNPs). The method used was the precipitation of silver as silver chloride (AgCl). Before precipitation, a prior 2 L filtration of the liquor from the second leaching stage of Route A was carried out with a 0.20 µm filtration membrane to eliminate possible wastes from previous leaching stages. For AgCl precipitation, NaCl was added (at 25 °C and constant agitation) twice in excess of the stoichiometric calculation, in the leached liquor, as Eq.(1):

$$AgSO_4(aq) + NaCl(s) \rightarrow AgCl(s)\downarrow + NaSO_4(aq) \quad (1)$$

Precipitation was identified by the formation of a white suspension salt (AgCl). The membrane-filtered liquor was stored and the material retained in the membrane was washed with high purity water and sent to dry at room temperature for 24 h. This dry material was weighed and analyzed by scanning electron microscopy coupled to dispersive energy spectroscopy (SEM/EDS) to identify the elements present in this precipitate obtained. The solubilization of this AgCl precipitate was carried out using ammonium hydroxide in the solid/liquid ratio of 1/30.

2.5. Synthesis of AgNPs

The method used for the synthesis of AgNPs has been described by Turkevich et al. [49] in which sodium citrate was used as a reducing and stabilizing agent at a concentration of 1% (v/v) or 10 g/L with reaction stoichiometry, as Eq.(2):

$$4Ag^+ + C_6H_5O_7Na_3 + H_2O \rightarrow 4Ag^0 + C_6H_5O_7H_3 + 3Na^+ + H^+ + O_2 \quad (2)$$

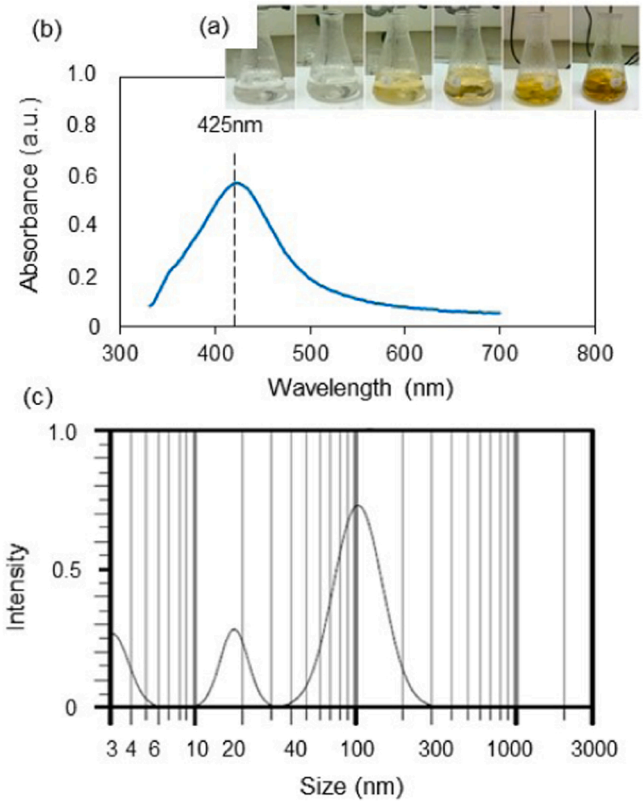

Fig. 13. a) Evolution of the AgNPs synthesis solution to 10 mL of sodium citrate and 25 min of hot stirring; b) UV–vis absorption spectra of the AgNPs synthesized (15.7 g.L-1 Ag, 25 min, sodium citrate drip 1%v/v), e c) Size distribution of AgNPs obtained by the DLS technique.

The solution containing Ag was placed in a 250 mL conical flask under heating, magnetic stirring (1100 rpm), and ORP control, with reference electrode Ag/AgCl, KCl mol.L^{-1}). This solution was brought to boiling, and sodium citrate was dropped (1 drop/second) onto it.

Synthesis tests of the nanoparticles were performed following parameters: volume of the reducing agent 5 mL, 10 mL and 15 mL; hot stirring time (after boiling) 15 min and 25 min. After removing the

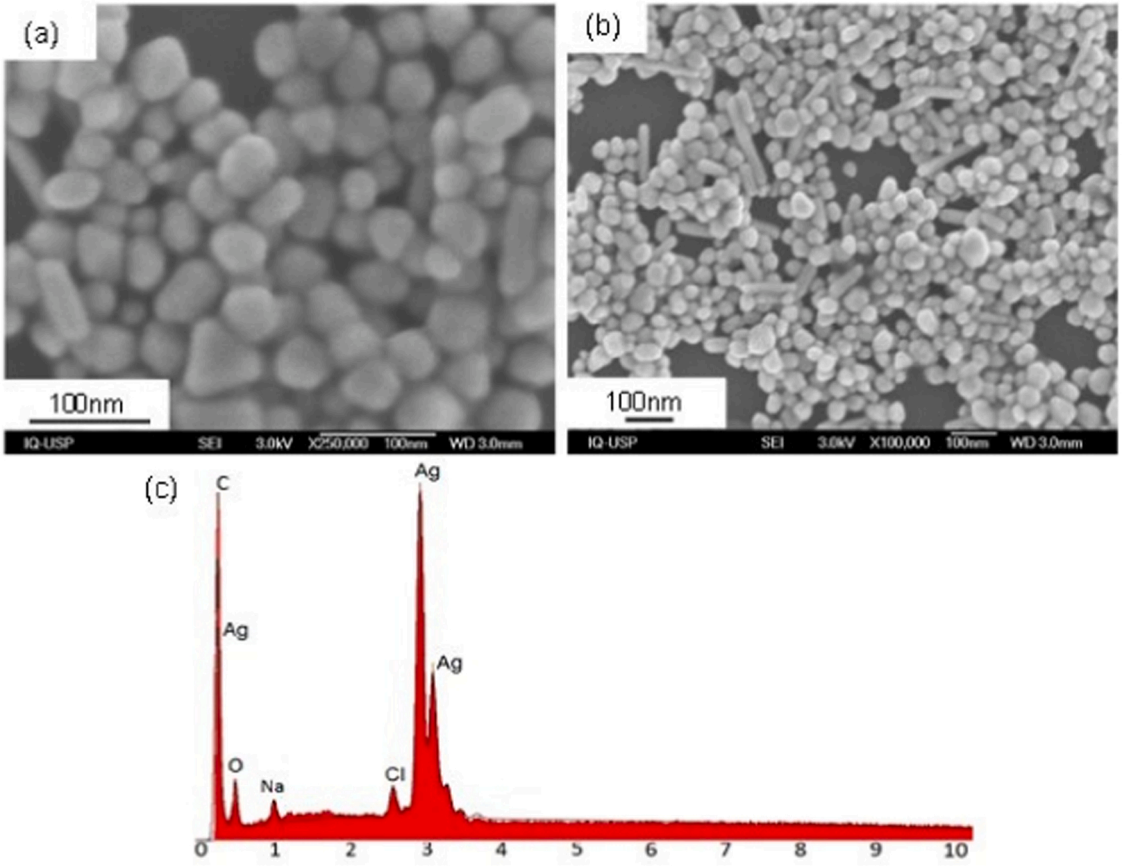

Fig. 14. FEG-SEM/EDS from the samples of AgNPs.

heating, the solution was kept under stirring at room temperature. This stirring (unheated) remained until the solution turned yellow. After stirring, the solution was left to stand at room temperature.

2.6. Characterization of AgNPs

The absorbance spectra of the synthesized nanoparticles were obtained by UV–vis absorbance spectroscopy (UV-Vis) in a Merck/Pharo 300 M spectrophotometer, with a wavelength range between 300 and 800 nm. Dynamic light scattering (DLS) analysis was performed to obtain the size distribution of the nanoparticles, using the Zetasizer Nano Series equipment. The morphology and composition of the nanoparticles produced were verified by field-scanning electron microscopy and dispersive energy spectroscopy (FEG-SEM/EDS) by the Jeol JSM-4701 F model.

2.7. Results and discussion

2.7.1. Characterization of the metals from WPCBs

The characterization results of the studied waste (with 96% of granulometry below 2 mm) showed that it contains: 0.053 wt% of Ag; 1.43 wt% of Al; 13.83 wt% of Cu; 1.47 wt% of Fe; 0.32 wt% of Ni; 1.70 wt% of Sn; and 0.043 wt% of Zn [37].

2.7.2. Metal recovery

Leaching conditions of each metal can be verified through the Pourbaix diagrams and they can vary with the concentration of the element and reaction temperature [50]. Thus, the Pourbaix diagrams of Cu, Fe, Ag, Al, Sn, Zn and Ni were evaluated for hydrometallurgical processing in which the pH and potential of the species subjected to the leaching process were correlated and evaluated individually (Fig. 1S–7S in Supplementary Material).

The potential (Eh) and pH conditions identified in Fig. 1S–7S (in the Supplementary Material) in which the metals could be present in the ionic or soluble phase were approximated to observe the specific conditions of leaching of these metals and, thus, favor (or not) selective leaching. These regions are represented in gray in the speciation diagrams and these leaching conditions are shown in Table 1.

The speciation diagrams of these metals in hydrochloric, sulfuric, and nitric acid were also observed to study the species that could be formed, in which "(c)" and "(M^{e+})" represent, respectively, the crystalline or solid phase and the metal in the soluble phase. Thus, depending on the metallic concentration, potential, pH, and anion that participates in the reaction, the study of selectivity in the extraction of each metal and the solubility of the species formed was carried out. Figs. 2–Fig. 8 shows the diagrams.

According to Fig. 2a), b) and c), Cu would form soluble species (Cu^{2+}, $CuCl^{+}$, $CuSO_4{}^{+}$, $CuNO_3{}^{+}$) below pH 6.5 in a nitric, hydrochloric, or sulfuric medium. Above this pH, the formation of an insoluble species of Cu (CuO) would be initiated therefore this pH condition was not considered favorable for the leaching of WPCBs. Although Cu is considered soluble in association with chloride, nitrate, and sulfate ions, in the sulfuric acid simulation (Fig. 2b), copper would have 85% dissolution at pH 0, and for the Cu^{2+} species, an increasing trend of dissolution is seen with increasing acid concentration. Thus, increasing the concentration of sulfuric acid to 2 M could reach 100% Cu leaching.

In the simulation of Fe leaching (Fig. 3a), its soluble phases (Fe^{3+}, $FeCl_2{}^{+}$) are observed in a hydrochloric medium below pH 0.5. In sulfuric medium (Fig. 3b), the soluble species ($FeSO_4{}^{+}$, $FeHSO_4{}^{2+}$, $Fe(SO_4)^{2-}$, $FeOH_2{}^{+}$) can be verified at pH below 2.3, and, in nitric medium ($FeOH_2$ +), Fig. 3c), the leaching pH is below pH 1.5. In all conditions of acid simulation, the predominance of insoluble phases (iron precipitate) is

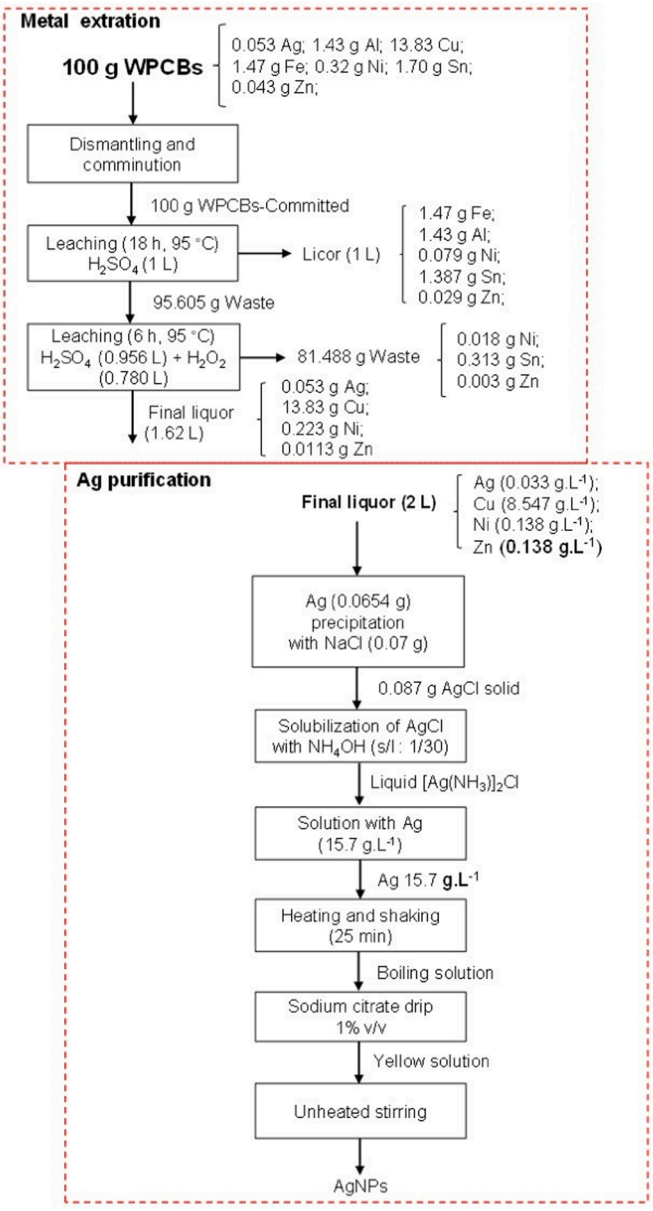

Fig. 15. Flowchart of the complete silver nanoparticle production route proposed from the recovery of Ag from WPCBs.

observed at pH above 2.

According to Fig. 4a), the Ag in hydrochloric medium would have about 93% of insoluble species (AgCl) in which (regardless of pH) about 5% of the species could form a metal complex ($AgCl^-$), depending on the other ions in the solution. In a sulfuric and nitric medium, Fig. 4b) and c), respectively, the Ag would be soluble up to pH 10.5 (according to the studied conditions). Ag precipitates would be formed between pH 10.5 and 12. Despite being soluble in nitric medium up to pH 10.5, the species formed would be silver nitrate, which may be photosensitive and degrades with light, forming silver oxide [51].

Fig. 5a), b) and c) show that 100% of the Al can be leached at pH below 3, and that it is precipitated between pH 5 and 8.5. In a hydrochloric medium, Al would become soluble as a metal complex ($Al(OH)^{4-}$) at a pH above 10, according to other ions in the solution. The results in the nitric medium are similar to those in the hydrochloric medium. In the sulfuric medium simulation, three soluble species could be observed up to pH 4.5 (Al^{3+}, $AlSO_4^+$, and $AlSO_4^{2-}$) and above pH 10 ($Al(OH)^{4-}$), and, between pH 5.5 and 8, insoluble fractions could be identified.

Sn (Fig. 6a, b, and c) would present soluble phases below pH 3 in the simulations of the three studied media. Above this pH, it would form insoluble species (independent of the associated anion), however, below pH 1, 100% of its leaching would be achieved.

The diagrams in Fig. 7a), b) and c) show the behavior of Zn that is similar for the three media evaluated. Soluble Zn species are identified at pH below 6. Between pH 9 and 11.5, insoluble Zn is in the form of hydroxide ($Zn(OH)_2$). At pH 0, all Zn can be leached in nitric media.

Through Fig. 8a), b) and c), we can see that the soluble species of Ni would present themselves at pH below 7.5, and the insoluble species would be identified from pH 8, for all the simulations carried out. Thus, as in the case of Zn, sulfuric media could leach all Ni at pH below 0.

Except for Ag, metals that were studied in the presence of hydrochloric media would form soluble chlorides. Therefore, the addition of chloride to the solution could promote the selective precipitation of Ag and its purification [23,32]. However, one of the problems with the use of hydrochloric acid would be its corrosive and toxic characteristics, such as with the generation of pollutants and gas emissions) [52].

According to the studies by Naseri Joda and Rashchi (2012), all nitrates are soluble at pH below 2. Thus, all metals evaluated would be leached under these conditions [41]. For the synthesis of AgNPs, this would not be interesting because larger amounts of contaminants (Cu, Fe, Sn, Ni, and Zn) would be in solution. Therefore, steps with sulfuric acid were employed.

The Pourbaix diagrams (Figs. 1S–7S in Supplementary Material) and. Table 1 also show the main interferences in the selective leaching of metals, such as Cu in the presence of Fe, in which the two metals would be leached. This fact can be explained by the Cu cementation process which is caused due to the presence of Fe and the difference in oxy-reduction potential between them [53]. The (3) (anode reaction), (4) (cathode reaction) and Eq. (5) (global reaction) describe this process [10,54]:

$$Fe_{(s)} \rightarrow Fe^{2+}_{(aq)} + 2e \quad (3)$$

$$Cu^{2+}_{(aq)} + 2e^- \rightarrow Cu_{(s)} \quad (4)$$

$$Fe_{(s)} + Cu^{2+}_{(aq)} \rightarrow Fe^{2+}_{(aq)} + Cu_{(s)} \quad (5)$$

Initial leaching (without the addition of peroxide or oxidizing agent) could be used to avoid the influence of Fe on Cu leaching [24,55]. The objective would be to favor the dissolution range of Fe using hydrochloric and/or sulfuric and/or nitric acid so the Cu would remain insoluble: pH 2.5–5. By adjusting the leaching conditions for the extraction of Fe, Zn would also become soluble. However, the presence of Zn in WPCBs in the form of alloys (such as brass) makes it difficult to extract them in isolation [56]. The Sn could also become soluble in the Fe extraction phase, as long as the working pH was below 0.5. This would happen with solutions above 1 M for nitric, sulfuric, and hydrochloric acids.

Studies of Yilmaz et al. also address the Ag cementation process by copper Eq. (6) [34]:

$$2Ag^+_{(aq)} + Cu^0_{(s)} \rightarrow 2Ag^0_{(s)} + Cu^{2+}_{(aq)} \quad (6)$$

The leaching conditions of Ag can be more influenced by Cu than with other metals found in the solution. The overlapping of the Pourbaix diagrams for Ag and Cu (25 °C) is shown in Fig. 9.

This overlap shows that Ag could be leached together with Cu. An alternative for selective leaching between these metals would be to leach Cu in an oxidizing medium. However, the reaction potential should be kept below 750 mV so the Ag would remain insoluble. After all the extraction and collection of the Cu leaching waste, the new leaching in oxidizing medium should be initiated, maintaining the potential above 750 mV. Thus, Ag in an aqueous medium could be obtained and the synthesis of nanoparticles of Ag could be performed.

2.8. Metal extraction liquor

Fig. 10 and Fig. 11 show the results of the percentage of leached mass in each stage of Route A and B, respectively, which were calculated in relation to the initial amount of metals present in the sample.

The main metal of interest in this study, Ag, was completely solubilized in the two routes (A and B) in which the reaction potential was maintained close to 750 mV. For Ag recovery from 100 g of WPCBs (containing 0.053 g of Ag) in Route A 0.053 g of Ag and, in Route B, 0.050 g were recovered. Thus, by comparing the two routes tested, acid leaching in sulfuric medium (1st of Route A) can be indicated for final solutions with lower concentrations of Fe and Al impurities since in this step 100% of these metals were leached, and it functioned as a purification stage for the removal of these metals. For applications that require a purified Cu, for example, Route B cannot contribute to the subsequent purification steps of this solution as all metals would also be in solution. These studies from different routes presented possibilities to recovery several interest metals only modifying the pH and ORP of the solutions.

The pH and ORP for each stage of Route A are represented in Table 2.

According to studies carried out through speciation and Pourbaix diagrams and the values presented in Table 2, the Fe, Al, Zn, and Ni could be solubilized in the first stage of leaching of Route A. In the second stage of the same route, Cu and Ag, as well as the remaining amount of Fe, Al, Zn and Ni could also be leached. Still, in the two stages, Sn would have the lowest percentage of solubilization, when compared to the other metals studied. After the final leaching, the Sn had the maximum recuperation of 81.6 wt% and 2.1 wt% in Route A and B, respectively.

2.9. Purification of silver

In the present study, the purification of the Ag involved unit chemical precipitation operations to extract the silver present in the extraction of liquor in salt form for later synthesis of AgNPs. After the hydrometallurgical processing, the liquor obtained was characterized in ICP-OES, in which the amount of Ag was analyzed with the result of 32.7 mg/L.

The amount of NaCl added was 0.07 g for 2 L of solution (excess of twice). After the addition of NaCl, the formation of a white precipitate in all the leached liquor was observed, as Fig. 12 a). The precipitate present in the membrane was analyzed in SEM/EDS, to check its composition, Fig. 12 b) and c).

Fig. 12 b) presents the electron scattered image of the precipitate adhered to the filtration membrane, after the chemical precipitation step. Fig. 12 c) shows the EDS of the microregion viewed in Fig. 12 b). Through the EDS, the composition of the precipitate present in the filtration membrane was observed, in which the presence of Ag, Cl and S was identified. The presence of S in the EDS can be justified using H_2SO_4 in the last stage of leaching of the waste. Cl and Ag, present in the EDS image, suggest the composition of the precipitate as AgCl. The other impurities have not been verified with the precipitated AgCl. Panda et al. also precipitated (also with AgCl) about 99% high purity Ag [57].

Upon solubilization of AgCl, Ag formed a metallic complex of diamine silver (I) chloride, according to Eq. (7).

$$AgCl + 2NH_4\,OH \rightarrow [Ag(NH_3)]_2Cl + 2\,H_2O \quad (7)$$

After solubilization of Ag as a diamine silver (I) chloride, a solution of concentration equal to 15.7 $g.L^{-1}$ was prepared, which was used for the synthesis of AgNPs. From the diammine silver (I) chloride, the silver nanoparticles can be synthesized using different reducing reagents, such as sodium borohydride [58], sodium citrate [59], ascorbic acid [60] e hydrazine [61]; and stabilizers, such as polyvinylpyrrolidone (PVP) and polyethylene glycol (PEG) [20] and cyclodextrin [62].

2.10. Synthesis and characterization of AgNPs

The formation of nanoparticles can be inferred by changing the color of the synthesis solution over time to yellow [63,64]. Therefore, the color changes of the final solutions and the formation/appearance of the precipitate were verified.

Table 3 presents the result of the AgNPs synthesis tests performed with the variation of the sodium citrate volume parameters and hot stirring time.

For the volumes of 5 and 15 mL of sodium citrate in the two times tested (15 and 25 min) the aspect of the solutions indicated that the AgNPs were not formed, as well as in the volume of 10 mL in the time of 15 min of hot stirring. According to the characteristic color and the non-formation of precipitate, the AgNPs were synthesized in the test in which the added volume of citrate was 10 mL and the time was 25 min

The evolution of the reaction and the color change of the solution are presented in Fig. 13 a).

The solution containing silver took about 25 min to change from translucent (onset of dripping) to light yellow, and an additional 5 min of cold stirring was maintained until a strong yellow color was obtained. The ORP value dropped from 524 mV (initial - after the end of the citrate drip) to 467 mV (final - after cold stirring and complete reduction of silver) indicating a reduction in silver and formation of nanoparticles [32,65].

Pillai and Kamat (2004) reported in their studies the control of the size and shape of the silver nanoparticles in the citrate ion reduction method in which the hot reaction time (of boiling) and the citrate concentration are important for the complete reduction of the Ag ions. They observed that by rapidly cooling the synthesis solution, only a partial reduction of the Ag ions occurs and that most of the reduction is completed with a higher concentration of citrate or an increase in the hot stirring process (boiling). Thus, these parameters interfere with the nucleation rate of the nanoparticles [66].

Blosi et al. stated that if the rate of reduction is slow only a few nuclei can be formed and the growth stage is increased, increasing in particle size. The particle dimensions can also increase if the reduction rate is rapid as in the tests performed with the addition of 15 mL of citrate (in excess) in which numerous nuclei can be formed, and nucleation would occur in both dissolution stages and crystallization [67].

Fig. 13 b) shows the UV–vis spectra for AgNPs synthesized where the absorbance peak is 425 nm which corresponds to the characteristic peak of AgNPs, confirming the observed staining results. Silver nanoparticles can present absorbance peaks around 400–420 nm [66,68,69].

The average size distribution was 67 nm and the histogram of the nanoparticle size distribution obtained through the DLS test showed as Fig. 13 c).: 68.6% of particles with an average diameter of 104.3 nm, 16.5% with an average diameter of 3 nm, and 14.9% of particles with 17.2 nm.

Fig. 14 a) and b) presents the image of secondary electrons and c) sample composition of AgNPs obtained by FEG-SEM/EDS. The presence of Cl and Na can be justified by the use of NaCl in the precipitation stage of Ag. After three washing cycles, the observation of two different regions of the sample indicated the morphology of the nanoparticles: morphology of spheres, rods and other shapes were observed with different dimensions.

Seerangaraj et al. synthesized AgNPs with an average size of 55.65 nm and also spherical. These AgNPs showed photocatalytic and biomedical degradation properties. Their nanoparticles exhibited potential bactericidal activity against *Gram-negative* and *Gram-positive* bacterial pathogens [70]. Thus, the application of nanoparticles prepared in this work can also be explored in different areas.

Fig. 15 shows a summary of the proposed complete route for the production of silver nanoparticles.

3. Conclusions

The studies of the speciation and Pourbaix (Fig. 1S–7S in Supplementary Material)-diagrams for each metal showed that different routes can be proposed for different metals of interest in WPCBs. The recovery of Ag from waste printed boards (memory boards) was proposed through two leaching routes in which 100% of the Ag and Cu were recovered in a solution without Al, Sn, and Fe, and a lower concentration of Ni and Zn was found after the 2nd leaching in an oxidizing sulfuric medium. This route can be used when a more purified solution of Ag and Cu is required. The Ag was purified by chemical precipitation with NaCl and its subsequent solubilization in NH_4OH. Thus, pure AgNPs with the average size distribution of 67 nm were synthesized by the Turkevich Method in 25 min. This work can be considered promising to make electronic waste a source for the production of high added value products (synthesis of recovered metal nanoparticles), as well as different applications of these nanoparticles. The present study also shows that the recycling of WPCBs can bring benefits in terms of the supply of raw resources, and it can contribute to the reduction of environmental pollution and risks to human health related to the incorrect release of dangerous substances into the environment, the concern with the depletion of mineral reserves, and the need to search for sources of secondary recovery of metals adding value to this waste.

CRediT authorship contribution statement

Marcos Paulo Kohler Caldas: Experiments, Conceptualization, Methodology, Investigation, Writing. **Thamiris Auxiliadora Gonçalves Martins:** Investigation, Conceptualization, Methodology, Writing. **Vivviane Tavares de Moraes:** Methodology, Visualization, Data curation, Writing – review & editing. **Jorge Alberto Soares Tenório:** Supervision, Review. **Denise Crocce Romano Espinosa:** Supervision, Writing – review & editing.

Declaration of Competing Interest

The authors declare the following financial interests/personal relationships which may be considered as potential competing interests: The authors wish to thank the Coordenaç ão de Aperfeiçoamento de Pessoal de N í vel Superior - Brasil (CAPES) - Finance Code 001, the University of Sao Paulo, the São Paulo Research Foundation (FAPESP) for financial support (Grant n○ 2019/11866-5, Grant nº 2012/51871–9 and Research Project 2018/07461-7), and Conselho Nacional de Desenvolvimento Científico e Tecnológico (CNPq) for financial support (Grant nº. 306936/2016-0).

Acknowledgment

This study was financed in part by the Coordenação de Aperfeiçoamento de Pessoal de Nível Superior - Brasil (CAPES) - Finance Code 001. The authors thank the University of Sao Paulo for all support, CAPES, the São Paulo Research Foundation (FAPESP), Brazil, for financial support (Grant n○ 2019/11866-5, Grant nº 2012/51871-9 and Research Project 2018/07461-7), and Conselho Nacional de Desenvolvimento Científico e Tecnológico (CNPq), Brazil, for financial support (Grant nº. 306936/2016-0).

Appendix A. Supporting information

Supplementary data associated with this article can be found in the online version at doi:10.1016/j.jece.2021.106845.

References

[1] N.V. Mdlovu, C.L. Chiang, K.S. Lin, R.C. Jeng, Recycling copper nanoparticles from printed circuit board waste etchants via a microemulsion process, J. Clean. Prod. 185 (2018) 781–796, https://doi.org/10.1016/j.jclepro.2018.03.087.
[2] S. Yousef, M. Tatariants, V. Makarevicius, S.-I. Lukošiūtė, R. Bendikiene, G. Denafas, A strategy for synthesis of copper nanoparticles from recovered metal of waste printed circuit boards, J. Clean. Prod. 185 (2018) 653–664, https://doi.org/10.1016/j.jclepro.2018.03.036.
[3] G.B. Vanessa Forti, Cornelis Peter Baldé, Ruediger Kuehr, The Global E-waste Monitor 2020: Quantities, flows and the circular economy potential., 2020. ⟨https://globalewaste.org⟩.
[4] C.P. Balde, F. Wang, R. Kuehr, J. Huisman, E-Waste Monitor, 2014.
[5] M. Tatariants, S. Yousef, S. Sakalauskaitė, R. Daugelavičius, G. Denafas, R. Bendikiene, Antimicrobial copper nanoparticles synthesized from waste printed circuit boards using advanced chemical technology, Waste Manag. 78 (2018) 521–531, https://doi.org/10.1016/j.wasman.2018.06.016.
[6] P. Hadi, M. Xu, C.S.K. Lin, C.W. Hui, G. McKay, Waste printed circuit board recycling techniques and product utilization, J. Hazard. Mater. 283 (2015) 234–243, https://doi.org/10.1016/j.jhazmat.2014.09.032.
[7] G.-H. Huynh, T.-L. Chen, C.-H. Hsu, Y.-H. Chen, P.-C. Chiang, Process integration of E-waste carbonization and High-gravity rotating packed bed for optimal gold recovery and the fine particles reduction, Sep. Purif. Technol. 241 (2020), 116686, https://doi.org/10.1016/j.seppur.2020.116686.
[8] A. Priya, S. Hait, Comparative assessment of metallurgical recovery of metals from electronic waste with special emphasis on bioleaching, Environ. Sci. Pollut. Res. 24 (2017) 6989–7008, https://doi.org/10.1007/s11356-016-8313-6.
[9] T. Havlik, D. Orac, M. Berwanger, A. Maul, The effect of mechanical-physical pretreatment on hydrometallurgical extraction of copper and tin in residue from printed circuit boards from used consumer equipment, Miner. Eng. 65 (2014) 163–171, https://doi.org/10.1016/j.mineng.2014.06.004.
[10] M. Kaya, Recovery of metals and nonmetals from electronic waste by physical and chemical recycling processes, Waste Manag. 57 (2016) 64–90, https://doi.org/10.1016/j.wasman.2016.08.004.
[11] A.C. Kasper, G.B.T. Berselli, B.D. Freitas, J.A.S. Tenório, A.M. Bernardes, H.M. Veit, Printed wiring boards for mobile phones: characterization and recycling of copper, Waste Manag. 31 (2011) 2536–2545, https://doi.org/10.1016/j.wasman.2011.08.013.
[12] C. Ning, C. Sze, K. Lin, D. Chi, W. Hui, G. Mckay, Waste printed circuit board (PCB) recycling techniques, Top. Curr. Chem. 375 (2017) 43, https://doi.org/10.1007/s41061-017-0118-7.
[13] J.V.J. Krishna, S.S. Damir, R. Vinu, Pyrolysis of electronic waste and their mixtures: kinetic and pyrolysate composition studies, J. Environ. Chem. Eng. 9 (2021), 105382, https://doi.org/10.1016/j.jece.2021.105382.
[14] A. Kuczy, E. Klugmann-Radziemska, Z. Sobczak, Recovery of silver metallization from damaged silicon cells, Sol. Energy Mater. Sol. Cells 176 (2018) 190–195, https://doi.org/10.1016/j.solmat.2017.12.004.
[15] S. Pérez-Martínez, J. Giro-Paloma, A. Maldonado-Alameda, J. Formosa, I. Queralt, J.M. Chimenos, Characterisation and partition of valuable metals from WEEE in weathered municipal solid waste incineration bottom ash, with a view to recovering, J. Clean. Prod. 218 (2019) 61–68, https://doi.org/10.1016/j.jclepro.2019.01.313.
[16] L. Amato A., F. Beolchini, Printed circuit board recycling: a patent review, J. Clean. Prod. 178 (2018) 814–832, https://doi.org/10.1016/j.jclepro.2018.01.076.
[17] R. Seif El-Nasr, S.M. Abdelbasir, A.H. Kamel, S.S.M. Hassan, Environmentally friendly synthesis of copper nanoparticles from waste printed circuit boards, Sep. Purif. Technol. 230 (2020), 115860, https://doi.org/10.1016/j.seppur.2019.115860.
[18] P.M.H. Petter, H.M. Veit, A.M. Bernardes, Evaluation of gold and silver leaching from printed circuit board of cellphones, Waste Manag. 34 (2014) 475–482, https://doi.org/10.1016/j.wasman.2013.10.032.
[19] G. Alvarado-Macías, J.C. Fuentes-Aceituno, F. Nava-Alonso, J. Lee, Silver leaching with the nitrite - copper novel system: a kinetic study, Hydrometallurgy 160 (2016) 98–105, https://doi.org/10.1016/j.hydromet.2015.12.014.
[20] B. Swain, D. Shin, S.Y. Joo, N.K. Ahn, C.G. Lee, J. Yoon, Selective recovery of silver from waste low-temperature co-fired ceramic and valorization through silver nanoparticle synthesis, Waste Manag. 69 (2017) 79–87, https://doi.org/10.1016/j.wasman.2017.08.024.
[21] B. Ghosh, M.K. Ghosh, P. Parhi, P.S. Mukherjee, B.K. Mishra, Waste printed circuit boards recycling: an extensive assessment of current status, J. Clean. Prod. 94 (2015) 5–19, https://doi.org/10.1016/j.jclepro.2015.02.024.
[22] M. Gurung, B.B. Adhikari, H. Kawakita, K. Ohto, K. Inoue, S. Alam, Recovery of gold and silver from spent mobile phones by means of acidothiourea leaching followed by adsorption using biosorbent prepared from persimmon tannin, Hydrometallurgy 133 (2013) 84–93, https://doi.org/10.1016/j.hydromet.2012.12.003.
[23] M. Sethurajan, E.D. van Hullebusch, D. Fontana, A. Akcil, H. Deveci, B. Batinic, J. P. Leal, T.A. Gasche, M. Ali Kucuker, K. Kuchta, I.F.F. Neto, H.M.V.M. Soares, A. Chmielarz, Recent advances on hydrometallurgical recovery of critical and precious elements from end of life electronic wastes - a review, Crit. Rev. Environ. Sci. Technol. 49 (2019) 212–275, https://doi.org/10.1080/10643389.2018.1540760.
[24] A. Tuncuk, V. Stazi, A. Akcil, E.Y. Yazici, H. Deveci, Aqueous metal recovery techniques from e-scrap: hydrometallurgy in recycling, Miner. Eng. J. 25 (2012) 28–37, https://doi.org/10.1016/j.mineng.2011.09.019.

[25] Q. Tan, L. Liu, M. Yu, J. Li, An innovative method of recycling metals in printed circuit board (PCB) using solutions from PCB production, (2019).
[26] L. Jing-ying, X. Xiu-li, L. Wen-quan, Thiourea leaching gold and silver from the printed circuit boards of waste mobile phones, Waste Manag 32 (2012) 1209–1212, https://doi.org/10.1016/j.wasman.2012.01.026.
[27] C. Lei, B. Yan, T. Chen, X.L. Wang, X.M. Xiao, Silver leaching and recovery of valuable metals from magnetic tailings using chloride leaching, J. Clean. Prod. (2018), https://doi.org/10.1016/j.jclepro.2018.01.243.
[28] N. Swain, S. Mishra, A review on the recovery and separation of rare earths and transition metals from secondary resources, J. Clean. Prod. 220 (2019) 884–898, https://doi.org/10.1016/j.jclepro.2019.02.094.
[29] J. Cui, L. Zhang, Metallurgical recovery of metals from electronic waste: a review, J. Hazard. Mater. 158 (2008) 228–256, https://doi.org/10.1016/j.jhazmat.2008.02.001.
[30] A. Ashiq, J. Kulkarni, M. Vithanage, Hydrometallurgical Recovery of Metals From E-waste, Elsevier Inc, 2019, https://doi.org/10.1016/B978-0-12-816190-6.00010-8.
[31] P.M.H. Petter, H.M. Veit, A.M. Bernardes, Evaluation of gold and silver leaching from printed circuit board of cellphones, Waste Manag 34 (2014) 475–482, https://doi.org/10.1016/j.wasman.2013.10.032.
[32] A. Khaleghi, S. Ghader, D. Afzali, Ag recovery from copper anode slime by acid leaching at atmospheric pressure to synthesize silver nanoparticles, Int. J. Min. Sci. Technol. 24 (2014) 251–257, https://doi.org/10.1016/j.ijmst.2014.01.018.
[33] Y.K. Yi, H.S. Kim, T. Tran, S.K. Hong, M.J. Kim, Recovering valuable metals from recycled photovoltaic modules, J. Air Waste Manag. Assoc. 64 (2014) 797–807, https://doi.org/10.1080/10962247.2014.891540.
[34] E. Yilmaz, S. Ertürk, F. Arslan, Silver recovery from dental amalgam wastes, Mater. Sci. Eng. Int. J. 3 (2019) 173–177, https://doi.org/10.15406/mseij.2019.03.00109.
[35] W.D. Xing, M.S. Lee, Leaching of gold and silver from anode slime with a mixture of hydrochloric acid and oxidizing agents, Geosystem Eng. 20 (2017) 216–223, https://doi.org/10.1080/12269328.2017.1278728.
[36] A. Behnamfard, M.M. Salarirad, F. Veglio, Process development for recovery of copper and precious metals from waste printed circuit boards with emphasize on palladium and gold leaching and precipitation, Waste Manag. 33 (2013) 2354–2363, https://doi.org/10.1016/j.wasman.2013.07.017.
[37] L.M. de Andrade, M.A. de Carvalho, M.P.K. Caldas, D.C.R. Espinosa, J.A.S. Tenório, Recovery of copper and silver of printed circuit boards from obsolete computers by one-step acid leaching, Detritus 14 (2021) 86–91, https://doi.org/10.31025/2611-4135/2021.14056.
[38] T.A.G. Martins, I.B.A. Falconi, G. Pavoski, V.T. de Moraes, M. dos, P. Galluzzi Baltazar, D.C.R. Espinosa, Green synthesis, characterization, and application of copper nanoparticles obtained from printed circuit boards to degrade mining surfactant by Fenton process, J. Environ. Chem. Eng. 9 (2021), 106576, https://doi.org/10.1016/j.jece.2021.106576.
[39] S. Yousef, M. Tatariants, M. Tichonovas, R. Bendikiene, G. Denafas, Recycling of bare waste printed circuit boards as received using an organic solvent technique at a low temperature, J. Clean. Prod. 187 (2018) 780–788, https://doi.org/10.1016/j.jclepro.2018.03.227.
[40] A. Marra, A. Cesaro, E.R. Rene, V. Belgiorno, P.N.L. Lens, Bioleaching of metals from WEEE shredding dust, J. Environ. Manag. 210 (2018) 180–190, https://doi.org/10.1016/j.jenvman.2017.12.066.
[41] N. Naseri Joda, F. Rashchi, Recovery of ultra fine grained silver and copper from PC board scraps, Sep. Purif. Technol. 92 (2012) 36–42, https://doi.org/10.1016/j.seppur.2012.03.022.
[42] V. Kumar, S. Singh, B. Srivastava, R. Bhadouria, R. Singh, Green synthesis of silver nanoparticles using leaf extract of Holoptelea integrifolia and preliminary investigation of its antioxidant, anti-inflammatory, antidiabetic and antibacterial activities, J. Environ. Chem. Eng. 7 (2019), 103094, https://doi.org/10.1016/j.jece.2019.103094.
[43] M. Sarkheil, I. Sourinejad, M. Mirbakhsh, D. Kordestani, Aquacultural engineering application of silver nanoparticles immobilized on TEPA-Den-SiO 2 as water filter media for bacterial disinfection in culture of penaeid shrimp larvae, Aquac. Eng. 74 (2016) 17–29.
[44] J.S. Kim, E. Kuk, K.N. Yu, J. Kim, S.J. Park, H.J. Lee, S.H. Kim, Y.K. Park, Y.H. Park, C. Hwang, Y. Kim, Y. Lee, D.H. Jeong, M. Cho, Antimicrobial effects of silver nanoparticles, nanomedicine nanotechnology, Biol. Med. 3 (2007) 95–101.
[45] C.N. Lok, C.M. Ho, R. Chen, Q.Y. He, W.Y. Yu, H. Sun, P.K.H. Tam, J.F. Chiu, C. M. Che, Silver nanoparticles: partial oxidation and antibacterial activities silver nanoparticles: partial oxidation and antibacterial activities, J. Biol. Inorg. Chem. 12 (2007) 527–534, https://doi.org/10.1007/s00775-007-0208-z.
[46] S.K. Gogoi, P. Gopinath, A. Paul, A. Ramesh, S.S. Ghosh, A. Chattopadhyay, Green fluorescent protein-expressing escherichia coli as a model system for investigating the antimicrobial activities of silver nanoparticles, Langmuir 22 (2006) 9322–9328.
[47] L.H. Yamane, V.T. de Moraes, D.C.R. Espinosa, J.A.S. Tenório, Recycling of WEEE: characterization of spent printed circuit boards from mobile phones and computers, Waste Manag. (2011) 2553–2558, https://doi.org/10.1016/j.wasman.2011.07.006.
[48] F.P.C. Silvas, M.M. Jiménez Correa, M.P.K. Caldas, V.T. de Moraes, D.C. R. Espinosa, J.A.S. Tenório, Printed circuit board recycling: physical processing and copper extraction by selective leaching, Waste Manag. 46 (2015) 503–510, https://doi.org/10.1016/j.wasman.2015.08.030.
[49] J. Turkevich, P.C. Stevenson, J. Hillier, A study of the nucleation and growth processes in the synthesis of colloidal gold, Discuss. Faraday Soc. 11 (1951) 55–75, https://doi.org/10.1039/DF9511100055.
[50] C.K. Gupta, Chemical Metallurgy Principles and Practice, Wiley, 2003, https://doi.org/10.1002/anie.200385071.
[51] Silver Nitrate Compound Summary, ⟨https://Pubchem.Ncbi.Nlm.Nih.Gov/Compound/24470#section=Structures⟩. (n.d.).
[52] Hydrochloric Acid Compound Summary, ⟨https://Pubchem.Ncbi.Nlm.Nih.Gov/Compound/313⟩ .2020. ⟨https://pubchem.ncbi.nlm.nih.gov/compound/313⟩.
[53] J.P.H. Perez, K. Folens, K. Leus, F. Vanhaecke, P. Van Der Voort, G. Du Laing, Progress in hydrometallurgical technologies to recover critical raw materials and precious metals from low-concentrated streams, Resour. Conserv. Recycl. 142 (2019) 177–188, https://doi.org/10.1016/j.resconrec.2018.11.029.
[54] E. Jackson, Hydrometallurgical Extraction And Reclamation, Ellis Horwood Ltd, N. Y., 1986.
[55] I. Birloaga, F. Vegliò, Study of multi-step hydrometallurgical methods to extract the valuable content of gold, silver and copper from waste printed circuit boards, J. Environ. Chem. Eng. 4 (2016) 20–29, https://doi.org/10.1016/j.jece.2015.11.021.
[56] L. Burzynska, Z. Zembura, Kinetics of spontaneous dissolution of copper-47.3 atom-% zinc brass with hydrogen depolarization slow reaction step, React. Solids 4 (1988) 373–381.
[57] R. Panda, M.K. Jha, D.D. Pathak, R. Gupta, Recovery of Ag, Cu, Ni and Fe from the nitrate leach liquor of waste ICs, Miner. Eng. 158 (2020), 106584, https://doi.org/10.1016/j.mineng.2020.106584.
[58] J.P. Oliveira, A.R. Prado, W.J. Keijok, M.R.N. Ribeiro, M.J. Pontes, B.V. Nogueira, M.C.C. Guimarães, A helpful method for controlled synthesis of monodisperse gold nanoparticles through response surface modeling, Arab. J. Chem. (2017), https://doi.org/10.1016/j.arabjc.2017.04.003.
[59] H.D. Beyene, A.A. Werkneh, H.K. Bezabh, T.G. Ambaye, Synthesis paradigm and applications of silver nanoparticles (AgNPs), a review, Sustain. Mater. Technol. 13 (2017) 18–23, https://doi.org/10.1016/j.susmat.2017.08.001.
[60] R. Phul, C. Kaur, U. Farooq, T. Ahmad, Ascorbic acid assisted synthesis, characterization and catalytic application of copper nanoparticles, Mater. Sci. Eng. Int. J. 2 (2018) 90–94, https://doi.org/10.15406/mseij.2018.02.00040.
[61] K.S. Tan, K.Y. Cheong, Advances of Ag, Cu, and Ag-Cu alloy nanoparticles synthesized via chemical reduction route, J. Nanoparticle Res. 15 (2013), https://doi.org/10.1007/s11051-013-1537-1.
[62] A. Khan, A. Rashid, R. Younas, R. Chong, A chemical reduction approach to the synthesis of copper nanoparticles, Int. Nano Lett. 6 (2016) 21–26, https://doi.org/10.1007/s40089-015-0163-6.
[63] J.L. Cholula-Díaz, D. Lomelí-Marroquín, B. Pramanick, A. Nieto-Argüello, L. A. Cantú-Castillo, H. Hwang, Synthesis of colloidal silver nanoparticle clusters and their application in ascorbic acid detection by SERS, Colloids Surf. B Biointerfaces 163 (2018) 329–335, https://doi.org/10.1016/j.colsurfb.2017.12.051.
[64] M.N. Haque, S. Kwon, D. Cho, Formation and stability study of silver nano-particles in aqueous and organic medium, Korean J. Chem. Eng. 34 (2017) 2072–2078, https://doi.org/10.1007/s11814-017-0096-z.
[65] J.I. Hussain, A. Talib, S. Kumar, S.A. Al-Thabaiti, A.A. Hashmi, Z. Khan, Time dependence of nucleation and growth of silver nanoparticles, Colloids Surf. A Physicochem. Eng. Asp. 381 (2011) 23–30, https://doi.org/10.1016/j.colsurfa.2011.02.048.
[66] Z.S. Pillai, P.V. Kamat, What factors control the size and shape of silver nanoparticles in the citrate ion reduction method? J. Phys. Chem. B 108 (2004) 945–951, https://doi.org/10.1021/jp037018r.
[67] M. Blosi, S. Albonetti, M. Dondi, C. Martelli, G. Baldi, Microwave-assisted polyol synthesis of Cu nanoparticles, J. Nanoparticle Res. (2011) 127–138, https://doi.org/10.1007/s11051-010-0010-7.
[68] K. Seah, T. Kuan, Y. Cheong, Advances of Ag, Cu, and Ag–Cu alloy nanoparticles synthesized via chemical reduction route, J. Nanopart. Res. (2013), https://doi.org/10.1007/s11051-013-1537-1.
[69] N.K.R. Bogireddy, H.A. Kiran Kumar, B.K. Mandal, Biofabricated silver nanoparticles as green catalyst in the degradation of different textile dyes, J. Environ. Chem. Eng. 4 (2016) 56–64, https://doi.org/10.1016/j.jece.2015.11.004.
[70] V. Seerangaraj, S. Sathiyavimal, S.N. Shankar, J.G.T. Nandagopal, P. Balashanmugam, F.A. Al-Misned, M. Shanmugavel, P. Senthilkumar, A. Pugazhendhi, Cytotoxic effects of silver nanoparticles on Ruellia tuberosa: photocatalytic degradation properties against crystal violet and coomassie brilliant blue, J. Environ. Chem. Eng. 9 (2021), 105088, https://doi.org/10.1016/j.jece.2021.105088.